complex with complete replacement of the oxalate ligands. In this case the same surface coordination is found as for the adsorption of the Cr(III) aquo complex.

The shape of the adsorption isotherm (Figure 5) after a short period of equilibration shows the expected reversal of the slope, i.e. the electrostatic anion adsorption on a positively charged surface. Increasing the equilibration time leads gradually to an inversion of the slope, which becomes stable after ca. 14 days. A comparison with the adsorption isotherm of the aquo complex (Figure 3) shows a smaller slope at 50% of adsorption. Furthermore, a significant shift of the adsorption isotherm to higher pH values is observed. From this it may be inferred that a new cationic surface complex has been formed.

The transition of the intermediate species is further characterized by ESEEM investigations. After 10 min the ESEEM spectrum is structured by the Larmor frequencies of the magnetic nuclei ^{27}Al and ^{1}H, as indicated by ν_{Al}, $2\nu_{Al}$, ν_H, and $2\nu_H$ (Figure 7). However, the spectrum is still dominated by the modulation of ambient protons resembling the case of $[Cr(C_2O_4)_3]^{3-}$ in solution. Simulation of aluminum ESEEM shows no significant difference for several types of coordination of metal ions to the hydrous oxide surface and gives no clear dependence of the geometrical parameters for various reasons.[7] The large spin quantum number $I = {}^5/_2$ of ^{27}Al causes the strong aluminum ESEEM, which can also be observed for long distances. Thus for a short equilibration time, the ESEEM spectroscopic data are indicative of an outer-sphere complex (Chart I) that is also supported by the ESR data (Figure 4).

After 14 days of equilibration time, the ESEEM spectra are dominated by the ^{27}Al frequency ν_{Al}. The broader features in the frequency domain are caused by the fast echo decay (Figure 8). This fast echo decay is interpreted to be due to the increased Cr^{3+}–Cr^{3+} dipolar interactions when inner-sphere surface complexes with ≡AlO functional groups are formed at high-density ligand exchange sites. An almost identical echo decay effect has been found for the adsorption of Cu^{2+} on δ-Al_2O_3[7] and can be taken as a supplementary evidence for surface complexations. The slow echo decay in Figure 7 on the other hand is indicative of an outer-sphere association; e.g. charge repulsion between Cr^{3+} ions leads to smaller dipolar interactions. The spectra support the finding concluded from the adsorption isotherm that the ligand replacement of $(C_2O_4)^{2-}$ has come to an equilibrium. The adsorption isotherm which is different from the one of $Cr(H_2O)_6{}^{3+}$ indicates that a new cationic surface complex has been formed. It is suggested that this surface complex consists of the $[Cr(C_2O_4)_x]^{3-2x}$ (x = 1, 2) moiety and the $[Cr(aq)]^{3+}$ fragment binding to the δ-Al_2O_3 surface (Chart II). A bidentate binding is proposed in analogy to previous findings with Cu^{2+}[7] and VO^{2+}[26] on δ-Al_2O_3.

Acknowledgment. This work was supported by a grant from the Board of the Swiss Federal Institute of Technology.

Contribution from the Department of Chemistry,
University of Wisconsin—Milwaukee, Milwaukee, Wisconsin 53201

Spectroscopic Evidence for a Centrosymmetric Dithionite Anion in the Solid State: Vibrational Spectroscopy of Tetraethylammonium Dithionite

William C. Hodgeman, Jeffrey B. Weinrach,[†] and Dennis W. Bennett*

Received March 28, 1990

Infrared and Raman spectroscopic studies of tetraethylammonium dithionite reveal that the dithionite anion adopts a staggered centrosymmetric configuration in the solid state, and in solution in both aqueous and nonaqueous solvents. This contrasts markedly with the structure of $S_2O_4{}^{2-}$ in salts containing the dithionite ion in the proximity of a relatively small cation, in which the ion adopts an anomalous "eclipsed" conformation. Moderate differences for lower energy vibrations are noted for $(Et_4N)_2S_2O_4$ in going from the solid state *or* nonaqueous solvents into aqueous solution. A normal-coordinate analysis of $S_2O_4{}^{2-}$ in $(Et_4N)_2S_2O_4$ resulted in a sulfur–sulfur bond stretch force constant of 1.3 mdyn Å^{-1}. The two Raman-active bands at 472 and 208 cm^{-1} consist of approximately equal contributions from the S–S bond stretch and S–S–O valence angle bend internal coordinates. There is no independent vibrational mode dominated by the S–S bond stretch internal coordinate, thus precluding the existence of a "sulfur–sulfur" group stretching frequency.

Introduction

From the time of its discovery in the early 1800s, the structure and chemistry of the common dithionite anion have sparked interest and stimulated debate.[1] On the basis of simple VSEPR considerations, the expected conformation for the $S_2O_4{}^{2-}$ ion should parallel the structures of other known sulfur–oxy anions containing sulfur–sulfur bonds, such as $S_2O_5{}^{2-}$ and $S_2O_6{}^{2-}$. In the absence of external perturbations, all three ions would be expected to adopt staggered configurations, with $S_2O_6{}^{2-}$ and $S_2O_4{}^{2-}$ belonging to centrosymmetric point groups D_{3d} and C_{2h}, respectively. As illustrated in Figure 1, $S_2O_5{}^{2-}$ and $S_2O_6{}^{2-}$ are "well-behaved" in this respect, with several crystal structures revealing the expected structures[2] and Raman spectra of their aqueous solutions indicating that the solvated ions are similar to those in the solid state.[3] The dithionite ion, however, stands in marked contrast to its cousins. In 1956 Dunitz reported the crystal structure of the disodium salt of the anion. This provided the first crystallographic evidence that it possessed approximate eclipsed C_{2v} symmetry and a surprisingly long sulfur–sulfur distance of 2.39 Å.[4] Subsequently, two other crystal structures of the dithionite anion have revealed the same anomalous structure.[5] The presence of $SO_2{}^-$ ions in solution and the solid state along with the strong reducing properties of dithionite salts has generally been attributed to this long and apparently weak sulfur–sulfur bond.

Even more striking are the changes that occur in the Raman spectrum of solid $Na_2S_2O_4$ (Figure 2a) when it is dissolved in aqueous solution (Figure 2b). These observations were published separately and independently by Peter and Meyer[6] and by Takahashi, Kaneko, and Miwa.[7] On the basis of polarized/depolarized Raman spectra and the mutual exclusion of Raman and

---

* To whom correspondence should be addressed.

[†] Current address: Los Alamos National Laboratory, Los Alamos, NM.

(1) Berzelius, J. J. *Lehrbuch der Chemie*; Dresden, Germany, 1825; p 472.

(2) (a) Zachariasen, E. A. *Phys. Rev.* **1932**, *40*, 923. (b) Lindqvist, I.; Mortsell, M. *Acta Crystallogr.* **1957**, *10*, 406. (c) Martinez, S.; Garcia-Blanco, S.; Rivoir, L. *Acta Crystallogr.* **1956**, *9*, 145.

(3) Sato, S.; Higuchi, S.; Tanaka, S. *Appl. Spectrosc.* **1985**, *39*, 822.

(4) Dunitz, J. D. *Acta Crystallogr.* **1956**, *9*, 579.

(5) (a) Kiers, C. T.; Vos, A. *Acta Crystallogr.* **1978**, *B34*, 1499. (b) Magnusson, A.; Johansson, L. *Acta Chem. Scand.* **1982**, *A36*, 429.

(6) Peter, L.; Meyer, B. *J. Mol. Struct.* **1982**, *95*, 131.

(7) Takahashi, H.; Kaneko, N.; Miwa, K. *Spectrochim. Acta* **1982**, *38A*, 1147.

0020-1669/91/1330-1611$02.50/0

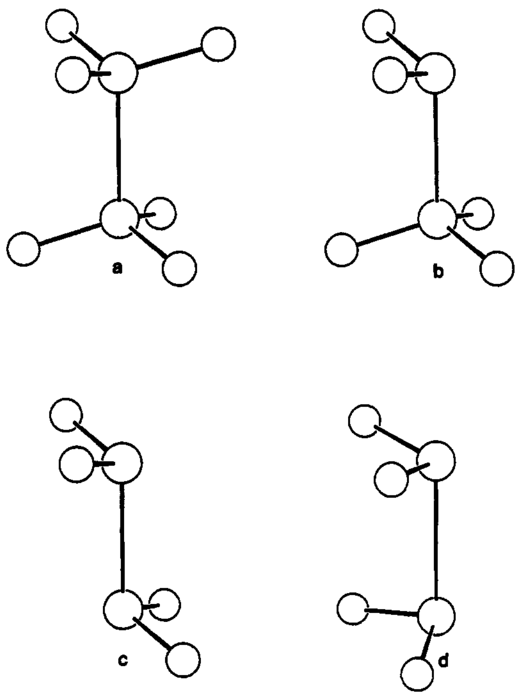

Figure 1. (a) Observed structure of $S_2O_6^{2-}$, (b) observed structure of $S_2O_5^{2-}$, (c) predicted structure of $S_2O_4^{2-}$, and (d) observed structure of $S_2O_4^{2-}$.

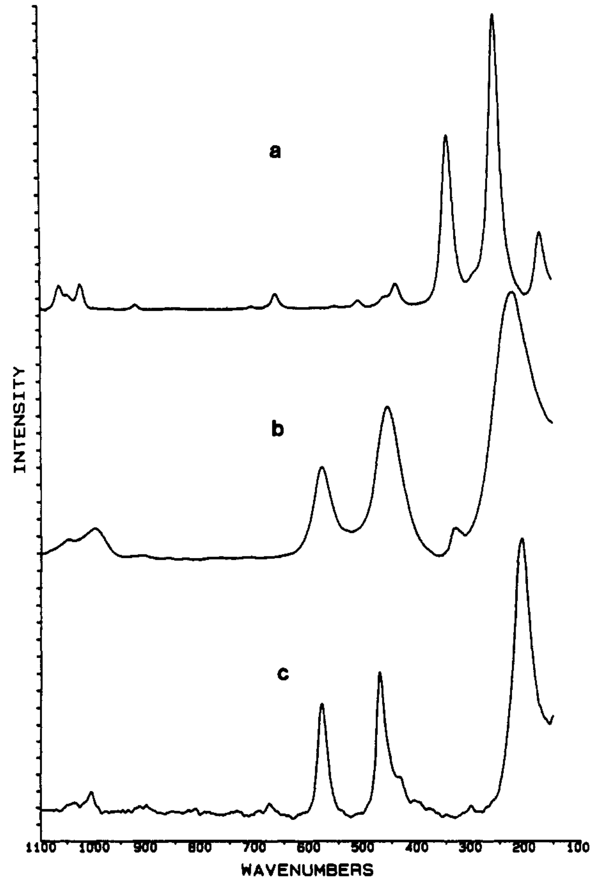

Figure 2. Raman spectra of (a) solid $Na_2S_2O_4$, (b) aqueous $Na_2S_2O_4$, and (c) solid $(Et_4N)_2S_2O_4$.

IR bands in the S–O stretching region, both groups concluded that the anion was centrosymmetric with C_{2h} symmetry in aqueous solution. Although Takahashi et al. acknowledged that the spectral differences could not be ascribed to a simple change of states, they concluded that the spectral shifts resulted from a change in the *symmetry* of the anion in going from the lattice environment to solution. Peter and Meyer took the argument one step further, postulating that the sulfur–sulfur bond length had also shortened, presumably due to a decrease in lone-pair electrostatic repulsions when the ion adopts the more stable staggered conformation.

Table I. Frequencies of Raman Bands (cm^{-1}) for $S_2O_4^{2-}$ in Water, Acetonitrile, Dimethyl Sulfoxide, and Dimethylformamide

H_2O	CH_3CN	$(CH_3)_2SO$	$(CH_3)_2NCHO$
1048	1055	1059^a	1052^a
1000	1011	1014	1010
584	580	580	579
460	472	471	471
324	303	...^{a}	305^a
228	208	208	208

^{a} Overlap with solvent bands.

The hypothesis proposed by Peter and Meyer is consistent with a careful study of the coordination environment of the cation in crystal structures of compounds containing the dithionite ion.[4,5] Although the number of ionic structures containing the $S_2O_4^{2-}$ ion is somewhat limited, in every case the oxygen atoms tend to orient preferentially, apparently to maximize electrostatic and/or coordinate–covalent interactions. This inevitably eclipses the nonbonded electron pairs on both sulfur atoms, potentially contributing to a weakening of the sulfur–sulfur bond. If this analysis is correct, then the eclipsed conformation and anomalously long sulfur–sulfur bond originate from Coulombic interactions in the lattice rather than intramolecular bonding forces, and it is likely that we will need to look elsewhere for a reason for the formation of SO_2^- radicals in solution or the prowess of dithionite as a reductant.

One important test of this hypothesis is the determination of the conformation of the anion in an ionic solid in which the size of the cation makes it difficult or impossible for the anion to adopt bidentate coordination about the cation. The synthesis of tetraethylammonium dithionite by Lough and McDonald[8] has provided us with such a compound. In this paper, we report the results of Raman and infrared spectroscopic studies of $(Et_4N)_2S_2O_4$ in both solution and the solid state and discuss these results in light of our understanding of the structure of the dithionite anion.

Experimental Section

Tetraethylammonium dithionite was generously provided by Dr. John McDonald at Battelle-Kettering Laboratory. Sodium dithionite was obtained from Virginia Chemicals, Inc., as their Virtex-D product and used without further purification. Solid-state infrared spectra, collected at 2-cm^{-1} resolution, were obtained as Nujol mulls on a computer-upgraded Nicolet MX-1 FTIR instrument. Nujol was stored over sodium prior to use to ensure dryness. Instrument accuracy was checked with standard polystyrene film. Raman spectra were recorded with a Spex 1401 double monochromator. The spectra were obtained as single scans and were smoothed with a locally written fast-Fourier-transform algorithm. The excitation source was a Coherent Model I-100-10 argon ion laser. Data were collected at 1-cm^{-1} resolution by using the 488-nm line at 400-mW power at the laser head. Slit widths were set at 400 μm. Scattering was measured at a back-scattering angle of 45° with respect to the incident beam. Positions of vibrational bands are reported relative to a calibration standard: the 217- and 315-cm^{-1} bands of CCl_4. Samples were handled under nitrogen, and solvents were dried and stored under nitrogen by using standard techniques. Raman samples were contained in melting point capillary tubes, sealed under nitrogen.

Results and Discussion

Raman and Infrared Spectroscopy. The solid-state Raman spectrum of $(Et_4N)_2S_2O_4$ is shown in Figure 2c. Unlike the marked changes observed for $Na_2S_2O_4$, the spectrum of the tetraethylammonium salt exhibits only broadening and modest shifts in the bands upon solvation, similar to the effects observed when $S_2O_5^{2-}$ and $S_2O_6^{2-}$ enter solution.[9] The Raman spectrum of solid tetraethylammonium dithionite is consistent with a C_{2h} conformation for the anion, with bands at 1041 cm^{-1} (B_g), 1005 cm^{-1} (A_g), 580 cm^{-1} (A_g), 472 cm^{-1} (A_g), 303 cm^{-1} (B_g), and 208 cm^{-1}

---

(8) Lough, S. M.; McDonald, J. W. *Inorg. Chem.* **1987**, *26*, 2024.

(9) Sato, S.; Higuchi, S.; Tanaka, S. *Appl. Spectrosc.* **1985**, *39*, 822.

Table II. Observed and Calculated Frequencies for $S_2O_4^{2-}$ and Potential Energy Contributions of Internal Coordinates

mode	freq, cm^{-1} obsd	freq, cm^{-1} calcd	contribution to potential energy, % S–S str	S–O str	O–S–O bend	S–S–O bend	O_2SSO_2 torsion
B_u	1058	1058		99.7			0.3
B_g	1041	1041		96.6		3.4	
A_g	1005	1005	0.1	93.7	5.5	0.7	
A_u	916	916		93.5	6.4	0.1	
A_g	580	579	4.9	0.6	93.5	1.0	
A_u	575	576		2.6	94.6	2.8	
A_g	472	472	46.5	3.4	4.1	46.0	
B_g	303	303		6.0		94.0	
A_u	...	297		0.2	2.4	97.4	
B_u	...	236		0.6		99.0	0.4
A_g	208	209	48.6		0.7	50.7	
B_u	...	171		0.3		0.3	99.4

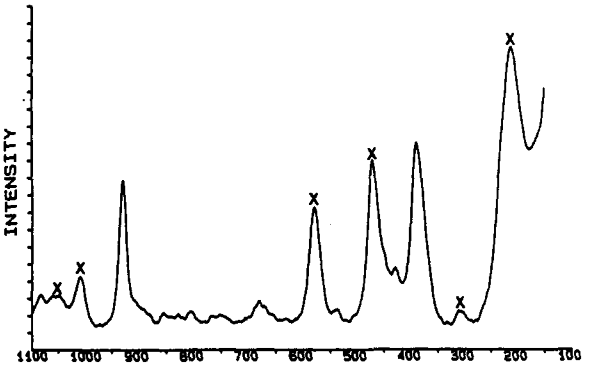

Figure 3. Raman spectrum of $(Et_4N)_2S_2O_4$ dissolved in acetonitrile. Peaks marked with an X are due to $S_2O_4^{2-}$.

(A_g). The low-intensity peak at 324 cm^{-1} in the spectrum of $S_2O_4^{2-}$ in aqueous solution, ascribed to a Raman-active mode with B_g symmetry,[7] is shifted to 303 cm^{-1} in the spectrum of solid $(Et_4N)_2S_2O_4$. Similarly, the intense band at 228 cm^{-1} in the spectrum of $Na_2S_2O_4(aq)$ is shifted to 208 cm^{-1} in the $(Et_4N)_2S_2O_4(s)$ spectrum.

The dithionite anion is expected to be strongly solvated in aqueous solution, probably through extensive hydrogen bonding. Differences in solid-state and solution spectra are usually ascribed to crystallographic packing forces, but as shown in Figure 3, the bands at 303 and 208 cm^{-1} do not shift when $(Et_4N)_2S_2O_4$ is dissolved in acetonitrile. The 303-cm^{-1} band is masked in dimethyl sulfoxide and dimethylformamide, but the lower frequency band is found at 208 cm^{-1} in both solvents (Table I). It is possible that spectra of $S_2O_4^{2-}$ in nonaqueous solvents appear shifted with respect to the spectrum of the anion in water because of significant ion pairing in the nonaqueous solvents, but it is highly unlikely that the shifts would be identical in all three cases. This indicates that the anion is less perturbed in nonaqueous solvents and in the solid state, supporting the hypothesis that the large cation makes preferential coordination unlikely. It is much more likely that the differences in spectra arise from the strong interaction of water molecules with excess negative charge on the oxygen atoms of the dithionite anion. This would serve to effectively "neutralize" excess charge density on the oxygen atoms in the anion through hydrogen bonding and thus reduce intramolecular electrostatic repulsion between the two SO_2 moieties.

The infrared spectrum of $(Et_4N)_2S_2O_4(s)$ is shown in Figure 4. The bands at 1058 and 916 cm^{-1} correspond to A_u and B_u modes, respectively, and were observed in the infrared spectrum of aqueous sodium dithionite.[7] The intense water absorbance masked other parts of the spectral region in the aqueous spectrum, but Takahashi et al. calculated the position of missing bands and *predicted* an IR absorbance band at 578 cm^{-1}. On the basis of observed spectra of Et_4NI, Et_4NBF_4, and $Et_4NCl{\cdot}2H_2O$, we have been able to tentatively assign all the peaks in the spectrum of Figure 4 to either Nujol (N) or the tetraethylammonium ion, with the exception of the intense band at 575 cm^{-1}. IR spectra of Et_4NI and Et_4NBF_4 are virtually featureless in the 550–650-cm^{-1} region of the spectrum, while $Et_4NCl{\cdot}2H_2O$ exhibits a minimum at about 575 cm^{-1} from the overlap of two intense peaks at 623/619 and 538 cm^{-1}. A number of bands were observed above 1100 cm^{-1} in both Raman and infrared spectra, all at higher frequencies than those associated with the S–O stretching region of the spectrum. They were therefore attributed to Nujol or the tetraethylammonium ion and did not enter into the analysis described herein. The assignment of the 575-cm^{-1} band as a dithionite ion vibrational mode (B_u) provides nine of twelve possible frequencies. The remaining frequencies are all IR active and are predicted to occur in the far-IR region of the spectrum. All bands in the Raman spectra of $(Et_4N)_2S_2O_4$ are absent in the observed infrared spectra and vice versa; this observation provides strong evidence that the $S_2O_4^{2-}$ ion is centrosymmetric in solution and *in solid tetraethylammonium dithionite.*

Table III. Internal Coordinate Force Constants for $S_2O_4^{2-}$ and $S_2O_5^{2-}$

int coord	force const, mdyn $Å^{-1}$ $(Et_4N)_2S_2O_4(s)$	$Na_2S_2O_4(aq)$[a]	$Na_2S_2O_5(aq)$[a]
S–S str	1.34	1.08	1.65
S–O str	6.30	6.15	6.15[b]
O–S–O bend	1.03	0.93	0.93[b]
S–S–O bend	0.32	0.32	0.32[b]

[a] Reference 6. [b] Thionite group.

Normal-Coordinate Analysis. Force constants were determined by using general vibrational analysis programs written by McIntosh and Peterson.[10] The programs employ the GF matrix method[11] and calculate normal-mode frequencies from user-input force constants corresponding to $3N - 6$ internal coordinates. Idealized coordinates for the ion were obtained by giving each SO_2 group the local geometry of the thionite group in the $S_2O_5^{2-}$ ion. Internal coordinates for the $S_2O_4^{2-}$ ion consisted of an S–S bond stretch, four S–O bond stretches, two O-S-O valence angle bends, four S–S–O valence angle bends, and one O_2S–SO_2 torsion. In addition to force constants for the internal coordinates, a number of interaction constants were also included. In general, interaction constants were determined for all internal coordinates that contained a common bond. Interaction constants were also determined for the S–O bond stretches on opposing sulfur atoms. The force constants were determined by initial estimations based on literature values,[7] followed by trial and error adjustments using the root-mean-square deviation (RMSD) between calculated and observed frequencies as a guide. Final force constant determination was effected using a SIMPLEX optimization least-squares fit,[12] resulting in a final RMSD of 0.605 cm^{-1}, within resolution limits of the Raman and infrared spectrometers. Observed and calculated frequencies and percentages of the potential energy distribution encompassed by the major contributing internal coordinates are given in Table II. Table III compares the force

---

(10) McIntosh, D. F.; Peterson, M. R. General Vibrational Analysis Programs. QCPE Program No. 342, University of Indiana, 1972.
(11) Wilson, E. B., Jr.; Decius, J. C.; Cross, P. C. *Molecular Vibrations*; McGraw-Hill: New York, 1955; Chapter 9.
(12) Nelder, J. A.; Mead, R. *Comput. J.* **1965**, *7*, 308.

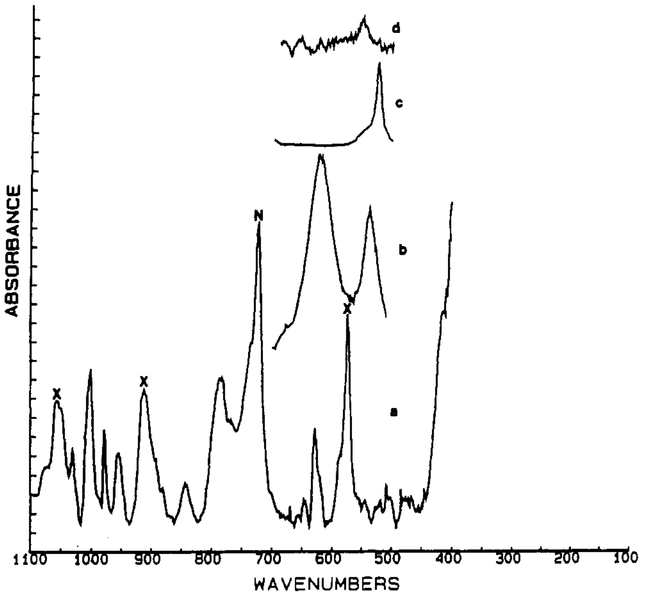

Figure 4. (a) Infrared spectrum of solid $(Et_4N)_2S_2O_4$. Peaks marked with an X are due to $S_2O_4^{2-}$. The peak labeled with N is due to Nujol. (b-d) Infrared spectra of (b) $Et_4NCl{\cdot}2H_2O$, (c) Et_4NBF_4, and (d) Et_4NI in the 500-700-cm^{-1} region.

constants for the internal coordinates for the $S_2O_4^{2-}$ and $S_2O_5^{2-}$ ions in aqueous solution (determined by Takahashi et al.) with those obtained for the dithionite ion in nonaqueous solvents and in solid $(Et_4N)_2S_2O_4$. The S-S bond stretch force constant is larger than that determined for the dithionite ion in aqueous solution but smaller than that for the metabisulfite ion. Previous investigators have assigned the band at 472[13] cm^{-1}, or alternatively the band at 208[6] cm^{-1}, as a "sulfur-sulfur" stretching frequency. The atom displacement vectors for these two vibrational modes suggest significant mixing of internal coordinates. The potential energy distributions for both normal modes indicate that each arises from approximately equal contributions from the sulfur-sulfur bond stretch and the S-S-O valence angle bends. There is therefore no vibrational mode which reflects an "independent" sulfur-sulfur stretching vibration. The torsion force constant is not included in the table, since the calculated frequency consists of a contribution from essentially one internal coordinate for which there are no observed data.

Concluding Remarks

Evidence for the existence of a centrosymmetric dithionite ion in aqueous solution[6,7] has been extended in this work to nonaqueous systems and the solid state. In all other known ionic crystal structures, the ion adopts a distorted eclipsed configuration, and we have hypothesized that this results from preferential orientation of the ion to maximize interaction with relatively small cations in the lattice. On the basis of this premise, it follows that the observed distortion of the ion results from crystallographic packing effects rather than intrinsic properties of the anion itself. The adoption of a "solution-like" conformation by the dithionite anion in an ionic solid that contains a cation large enough to minimize the effects of such preferential orientation provides strong support for this hypothesis.

Acknowledgment. We wish to thank Dr. John McDonald for the tetraethylammonium dithionite used in this work. D.W.B. and J.B.W. acknowledge support from Virginia Chemicals, Inc.

Registry No. $(Et_4N)_2S_2O_4$, 108563-02-6.

---

(13) Simon, A.; Kuchler, H. *Z. Anorg. Chem.* **1949**, *260*, 161.

Contribution from the Dipartimento di Chimica Inorganica, Chimica Fisica e Chimica dei Materiali,
Università di Torino, Via P. Giuria 7, 10125 Torino, Italy, and Chemistry Center,
Instituto Venezolano de Investigaciones Cientificas, Apartado 21827, Caracas 1020-A, Venezuela

^{1}H Spin-Lattice NMR Relaxation Studies of Hydride Carbonyl Clusters. A Method To Evaluate Distances Involving Hydrido Ligands

Silvio Aime,*[†] Marco Cisero,[†] Roberto Gobetto,[†] Domenico Osella,[†] and Alejandro J. Arce[‡]

Received September 14, 1989

Proton longitudinal relaxation rates of hydride resonances are dominated by the dipolar interaction with other ^{1}H nuclei in the same molecule and may provide relevant structural information once the molecular correlation times are determined by independent experiments. H-H distances were determined by this route in $HOs_3(CO)_{10}(O_2CH)$ (I), $HOs_3(CO)_9C_2H$ (II), and $HOs_3(CO)_{10}OH$ (III), whose resonances are well separated in their ^{1}H NMR spectra. When the proton NMR spectrum of compound III is recorded in acetone, it shows a mixture of two different isomers differing in the orientation of the lone pair on the μ-oxygen atom, as revealed by a marked difference in the relaxation times of the hydride ligands. Furthermore, an alternative procedure based on the comparison of the proton relaxation rates between H,H and H,D isotopomers has been applied for the dihydride species $H_2Os_3(CO)_{10}$ (IV), $H_2FeOs_3(CO)_{13}$ (V), and $H_2FeRu_3(CO)_{13}$ (VI), where the hydride ligands are chemically equivalent.

Introduction

NMR spectroscopy has become one of the most successful analytical techniques for transition-metal carbonyl hydrides, since ^{1}H resonances of these ligands fall in a characteristic region (-5/-20 ppm) upfield of TMS,[1] allowing their rapid and unambiguous characterization. Few exceptions to this general rule have been reported until now, and their observation is consistent with an early theoretical treatment of δ_H forwarded by Buckingham and Stephens.[2]

Couplings too are very useful in the assignment of stereochemical properties of hydride complexes both with nuclei on other ligands and with magnetically active metals.[3]

Relaxation properties have not been deeply investigated, yet nevertheless their determination can be of high potential value in the elucidation of the structural and dynamic features of these species.[4]

[†] Università di Torino.

[‡] Instituto Venezolano de Investigaciones Cientificas.

(1) See, for example: Kaesz, H. D.; Saillant, P. B. *Chem. Rev.* **1972**, *72*, 231. Humphries, A. P.; Kaesz, H. D. *Prog. Inorg. Chem.* **1979**, *25*, 145.

(2) Buckingham, A. D.; Stephens, P. J. *J. Chem. Soc.* **1964**, 2747; **1964**, 4583.

(3) (a) Mann, B. E.; Masters, C.; Shaw, B. L. *Chem. Commun.* **1970**, 1041. (b) Vander Velde, D. G.; Holmgren, J. S.; Shapley, J. R. *Inorg. Chem.* **1987**, *26*, 3077. (c) Koridze, A. A.; Kizas, O. A.; Kolobova, N. E.; Petroskii, P. V.; Fedin, E. I. *J. Organomet. Chem.* **1984**, *265*, C33. (d) Holmgren, J. S.; Shapley, J. R.; Belmonte, P. A. *J. Organomet. Chem.* **1985**, *284*, C5. (e) Constable, E. C.; Johnson, B. F. G.; Lewis, J.; Pain, G. N.; Taylor, H. J. *J. Chem. Soc., Chem. Commun.* **1982**, 754. (f) Cabeza, J. A.; Mann, B. E.; Brevard, C.; Maitlis, P. M. *J. Chem. Soc., Chem. Commun.* **1985**, 65. (g) Cabeza, J. A.; Mann, B. E.; Maitlis, P.; Brevard, C. *J. Chem. Soc., Dalton Trans.* **1988**, 629.

0020-1669/91/1330-1614$02.50/0